



Ab initio molecular dynamics simulation on stress reduction mechanism of Ti-doped diamond-like carbon films



Xiaowei Li, Peiling Ke, Aiyang Wang*

Key Laboratory of Marine Materials and Related Technologies, Zhejiang Key Laboratory of Marine Materials and Protective Technologies, Ningbo Institute of Materials Technology and Engineering, Chinese Academy of Sciences, Ningbo 315201, PR China

ARTICLE INFO

Available online 3 December 2014

Keywords:

Diamond-like carbon
Titanium doping
Compressive stress
Ab initio molecular dynamics

ABSTRACT

Structural properties of Ti-doped diamond-like carbon (DLC) films as a function of Ti concentrations (1.56–7.81 at.%) were investigated by ab initio molecular dynamics simulation to clarify the stress reduction mechanism. Results showed that with introducing Ti into DLC films, the residual compressive stress decreased firstly and then increased, which was consistent with the previous experimental results. Structural analysis revealed that the addition of Ti efficiently relaxed both the highly distorted bond angles and bond lengths, which led to the reduction of residual stress; the increase of residual stress at the high Ti concentration was attributed to the existence of distorted Ti–C structures and the increased fraction of distorted C–C bond lengths.

© 2014 Elsevier B.V. All rights reserved.

1. Introduction

Diamond-like carbon (DLC) films have attracted extensive interests both from scientific disciplines and industrial societies due to their unique structures and excellent mechanical, electronic, optical, as well as the magnetic properties [1–4], which make them not only used as a protective coating in various industrial applications, but also considered in the fields of solar cells, data storages, biomedical implants etc. [5–7]. However, high level of residual compressive stress formed in the deposition limits the films thickness to a few tens of nanometers and is the major drawback for their technological applications. Recently, it has been shown experimentally that an effective way to decrease the high residual stress of DLC films is the addition of a certain amount of metal elements such as Ti, Cr, W, Ni, Cu, or Ag during the growth process [8–13]. For example, doping Ti, W, or Cr into amorphous carbon matrix decreased the stress without serious deterioration of hardness because of the partly formed hard carbide nano-particulates, increased sp^2 graphitization, C- sp^3 substitution by doped transition metal atoms as well as the proposed pivot relaxation role [8,9]. It is well known that the residual stress strongly depends on the distorted atomic bonds of amorphous carbon systems. However, the addition of metal atoms brings the complexity of film structure. Especially, due to the limited experimental characterization of the atomic bond structure, the effect of doped metal atoms on the atomic bond structure from the viewpoint of atomic scale is yet to be clarified, leading to the phenomenological explanation of stress reduction mechanism.

In the present work, ab initio molecular dynamics (AIMD) simulation based on the density functional theory (DFT) was carried out to

study the structure and properties of Ti-doped DLC (Ti-DLC) films. The Ti concentration was changed from 1.56 to 7.81 at.%. The radial distribution function (RDF), properties including the residual compressive stress and bulk modulus, and both the bond angle and bond length distributions were evaluated to reveal the dependence of structural properties on Ti concentrations and finally to elucidate the stress reduction mechanism. Results showed that the structural evolution was strongly dominated by the concentrations of the doped Ti atoms, which provided the explanations for the changes in the physicochemical properties of Ti-DLC films.

2. Computational details

The structural models for Ti-DLC films were generated from liquid quench by AIMD simulation, which has been demonstrated to give a good description of DLC materials and reveal the intrinsic relation between the structure and properties [14–17]. The Vienna ab initio simulation package [18,19] based on the DFT was employed for the spin-polarized calculations with a cutoff energy of 500 eV, a generalized gradient approximation with the Perdew–Burke–Ernzerhof parameterization [20], a Gaussian smearing factor of 0.05 eV and a gamma point. The periodic boundary conditions were imposed on the supercell. In this work, the initial configuration contained 64 atoms in a simple cubic supercell with constant volume throughout the simulation. To obtain Ti-doped amorphous structures, the systems were firstly equilibrated at 8000 K for 1 ps using a canonical ensemble with a Nose thermostat to become completely liquid and eliminate their correlation to the initial configurations. Then the samples were cooled down to 1 K within 0.5 ps, corresponding to a cooling rate of 1.6×10^{16} K/s. After that, geometric optimization was performed using conjugated gradient method [21], in which a self-consistent field was created using an

* Corresponding author. Tel.: +86 574 86685036; fax: +86 574 86685159.
E-mail address: aywang@nimte.ac.cn (A. Wang).

energy convergence criterion of 10^{-5} eV, and atomic relaxation was repeated until the forces acting on the atoms were below 0.01 eV/Å.

Five samples were obtained at each density (2.03 or 2.87 g/cm³) with various Ti concentrations (1.56–7.81 at.%, corresponding to 1, 2, 3, 4 and 5 Ti atoms in 64-atom systems, respectively). In order to provide more representative models of the real Ti-DLC system than the direct substitution of carbon by Ti atoms in previously generated pure DLC networks, Ti atoms were introduced by substituting carbon atoms in the liquid carbon system [16]. Pure DLC films were also involved for comparison with Ti-doped ones. Before characterizing the structure and coordination number of Ti-DLC films, the RDF, $g(r)$, in the Ti-DLC system with high Ti concentration (39 at.%) was analyzed firstly to define the Ti and C atoms being bonded or non-bonded with each other. The distance to the first minimum in RDF was set as the cutoff distance, R_{cut} , for C–C of 1.85 Å, C–Ti of 2.56 Å, or Ti–Ti of 3.51 Å [22,23].

3. Results and discussion

Fig. 1 shows the final morphologies for pure-DLC and Ti-DLC films with the Ti concentrations of 1.56, 3.13 and 7.81 at.% at 2.87 and 2.03 g/cm³, respectively. Red spheres represent the carbon atoms while purple ones are Ti atoms. All the films are amorphous as will be described later by RDF. It is noted that comparing with the pure-DLC film at 2.87 g/cm³, the low-density structure of pure-DLC film (2.03 g/cm³) is looser and contains many planar chains which are weakly cross-linked; as the density changes to 2.87 g/cm³, the sp^3 C content increases to 56.25% from 15.62%. After the addition of Ti, the sp^3 hybridized structure with the Ti concentration increases gradually and then decreases for each case. Taking the Ti-DLC films at 2.87 g/cm³ for example (Fig. 1a), when the Ti concentration is 3.13 at.%, the maximal sp^3 C content reaches to 71.88%. This is attributed to the doped Ti atoms that could easily bond with the sp^2 C atoms with low bonding energy, which agrees well with the experimental results [8]. With further increasing Ti concentration to 7.81 at.%, many highly distorted five-coordinated C atoms with the content of 14.06% are generated, causing the decrease of sp^3 C content and also the existence of many distorted C–C and C–Ti atomic bond structures which would produce the high residual compressive stress.

Fig. 2 shows the RDF spectra of pure-DLC and Ti-DLC films with different Ti concentrations, in which the vertical dotted lines represent the 1st and 2nd nearest peak positions of crystalline diamond. It reveals that for each case the film exhibits the typical amorphous character that is long-range disorder and short-range order. Firstly, for pure-DLC films, the 1st C–C nearest neighbor peak with increasing the density is displaced from 1.46 Å at 2.03 g/cm³ to 1.50 Å at 2.87 g/cm³, which is

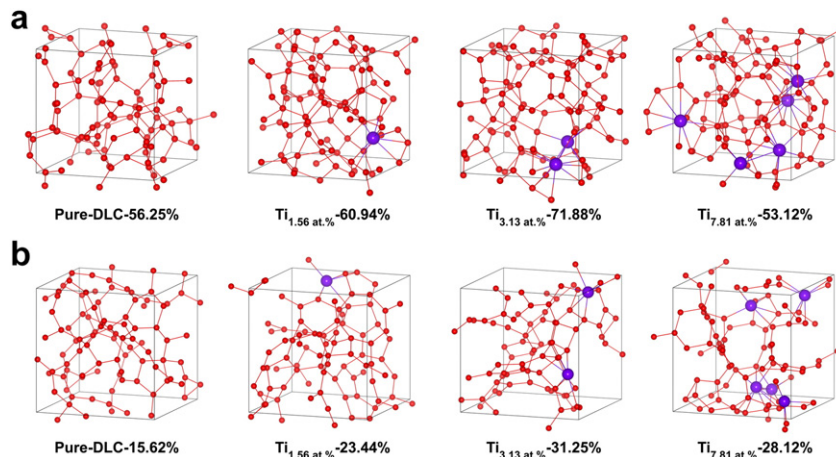


Fig. 1. Atomic structure of pure-DLC and Ti-DLC films with Ti concentrations of 1.56, 3.13, and 7.81 at.% at densities of (a) 2.87 g/cm³ and (b) 2.03 g/cm³, where the numbers are the sp^3 C contents in each film, and red, purple colors indicate the C and Ti atoms, respectively.

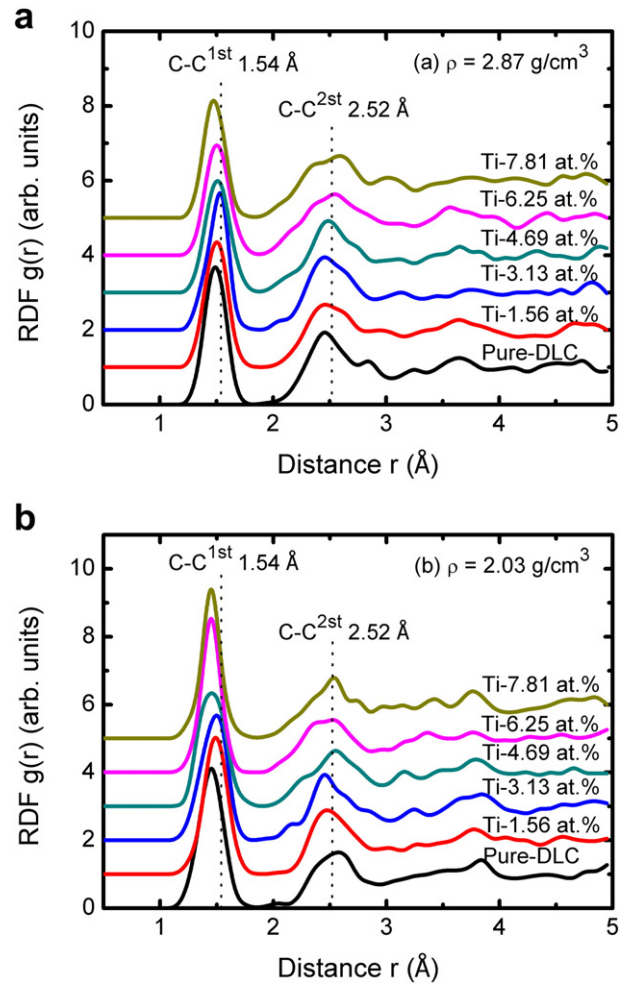


Fig. 2. RDF spectra of pure-DLC and Ti-DLC films with different Ti concentrations at densities of (a) 2.87 or (b) 2.03 g/cm³, respectively. The vertical dotted lines represent the 1st and 2nd nearest peak positions of crystalline diamond.

well consistent with the previous experimental [24,25] and theoretical results [16], suggesting that the simulated results represent the nature of real system. In general, the 1st peak is related with the atomic bond lengths, and the 2nd peak has correlation with both the bond angles and bond lengths. However, after the addition of Ti into DLC films, the

positions of the 1st and 2nd nearest neighbor peaks in Ti-DLC films at 2.87 or 2.03 g/cm³ are deviated from that of pure-DLC films, demonstrating the evolution of atomic bond structure which may play a key role on the properties of films.

The dependence of the calculated residual compressive stress and bulk modulus on the Ti concentrations is illustrated in Fig. 3. The pure-DLC film at 2.87 g/cm³ shows a high residual compressive stress of about 17.7 GPa, while the tensile stress of about 1.7 GPa is generated in the low-density pure-DLC film (2.03 g/cm³). With introducing Ti atoms into the films at 2.87 g/cm³ as shown in Fig. 3a, the compressive stress as the Ti concentrations decreases drastically and then increases; when the Ti concentration is 1.56 at.%, the minimal residual compressive stress of about 9.4 GPa is obtained, which is reduced by 46.9% comparing with the pure case; as the Ti concentration further reaches up to 7.81 at.%, the compressive stress increases to 20.4 GPa. Similar tendency of experimental results has been proved in previous study [8]. Besides, Fig. 3a also reveals that the addition of Ti (1.56–7.81 at.%) doesn't make obvious change to the bulk modulus. In the Ti-DLC films at 2.03 g/cm³ (Fig. 3b), the evolutions of residual stress and bulk modulus as a function of Ti concentrations are similar to that at 2.87 g/cm³.

In order to gain insight into the structural evolution in terms of Ti concentrations and elucidate the stress reduction mechanism, the atomic bond structure was analyzed. Taking the Ti-DLC films with the density of 2.87 g/cm³ representatively to explore the relation between the atomic bond structure and the significant reduction of residual stress (Fig. 3), Fig. 4 shows the bond angle and length distributions for pure-DLC and Ti-DLC films with the Ti concentrations of 1.56 and 7.81 at.%, respectively. The inset in Fig. 4a is the total bond angle distribution which is mainly composed of C–C–C, C–Ti–C, and C–C–Ti bond angles, and the inset in Fig. 4b is the total bond length distribution which mainly consists of C–C, and C–Ti bond lengths. From the insets of

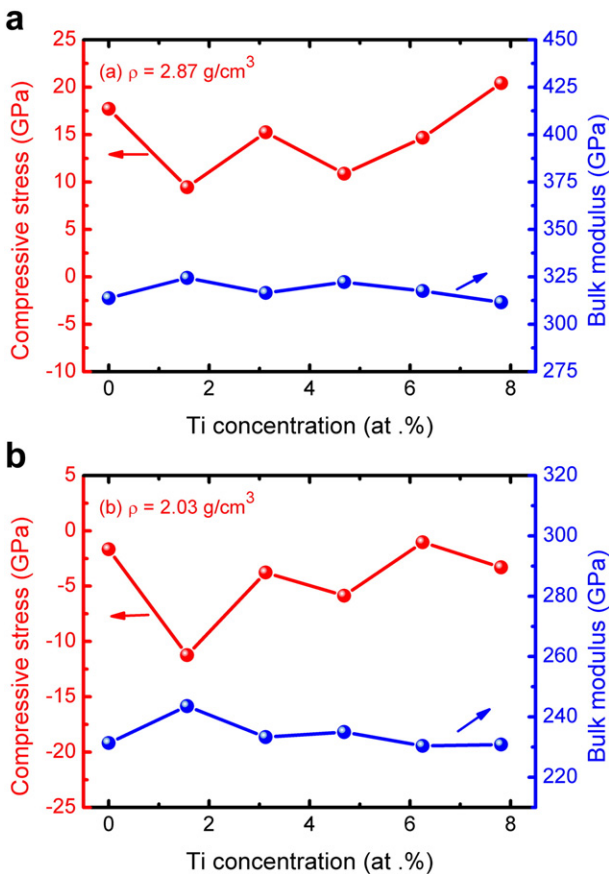


Fig. 3. Compressive stress and bulk modulus of Ti-DLC films as a function of Ti concentrations at densities of (a) 2.87 g/cm³ or (b) 2.03 g/cm³, respectively.

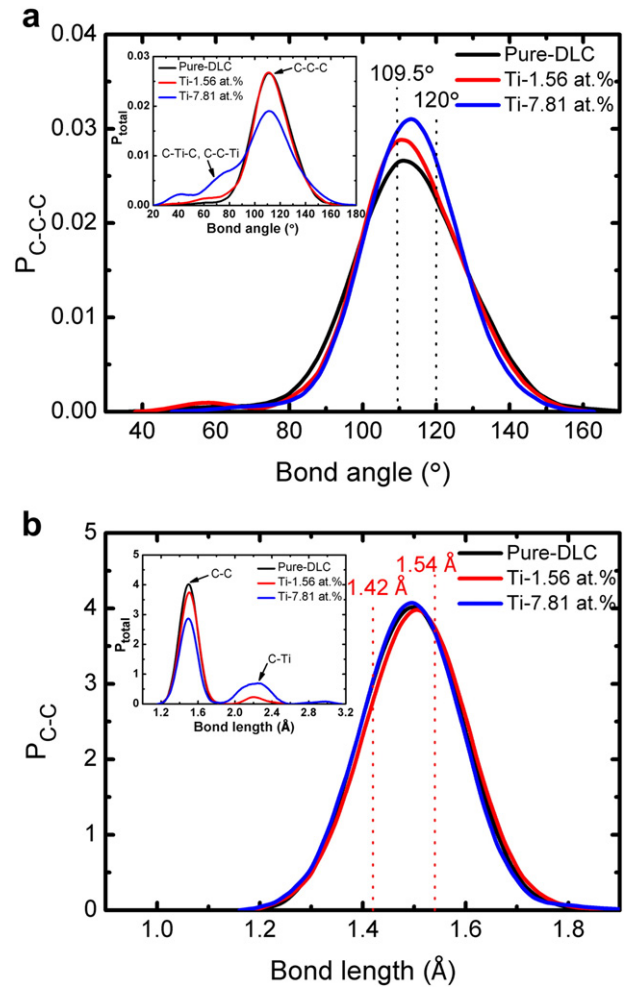


Fig. 4. Bond angle and length distribution functions of Ti-DLC films at 2.87 g/cm³ (a) Bond angle distribution, P_{C-C-C}, in which black dotted lines represent the stable bond angle of 120° for graphite and the one of 109.5° for diamond, and the inset is the total bond angle distribution mainly being composed of C–C–C, C–Ti–C, and C–C–Ti bond angles. (b) C–C bond length distribution, P_{C-C}, in which red dotted lines represent the stable bond length of 1.42 Å for graphite and the one of 1.54 Å for diamond, and the inset is the total bond length distribution, mainly being composed of C–C, and C–Ti bond length.

Fig. 4, it shows that following the Ti concentrations, the peak value of the total bond angle distribution (inset in Fig. 4a) decreases and the peak width shifts toward the small bond angles obviously, which are induced by the existence of C–Ti–C and C–C–Ti bond angles; in the total bond length distribution (inset of Fig. 4b), a small peak located at around 1.85–2.5 Å is generated, which mainly originates from C–Ti bond because it is longer than C–C bond.

Li et al. [26] reported that the high residual compressive stress in DLC films mainly originated from the distortion of both the bond angles and bond length of carbon network which were less than 109.5° and 1.42 Å, respectively. So we focused on the C–C–C bond angles and C–C bond length in particular. By integrating the C–C–C bond angle and C–C bond length distributions (Fig. 4a–b), the fractions of distorted bond angles (<109.5°) and bond lengths (<1.42 Å) in pure-DLC and Ti-DLC films with Ti concentrations of 1.56 and 7.81 at.% are thus deduced separately, as shown in Fig. 5. When the Ti concentration increases from 0 to 1.56 at.%, the fractions of both the highly distorted bond angles (<109.5°) and the bond length (<1.42 Å) are reduced simultaneously, leading to the decrease of residual compressive stress of DLC films in Fig. 3a. But in Ti-DLC film with the Ti concentration of 7.81 at.%, the fraction of distorted C–C bond length increases significantly; taking into account

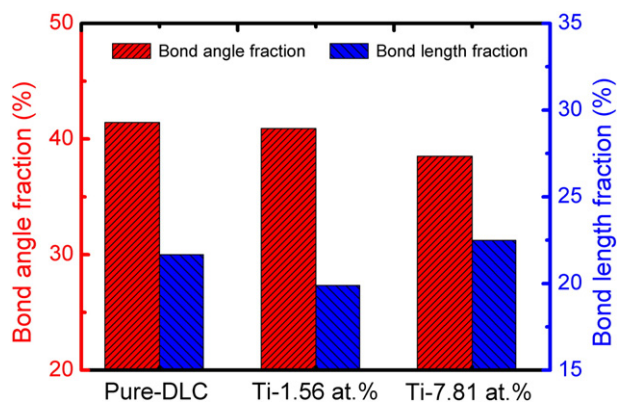


Fig. 5. Fractions of distorted bond angles ($<109.5^\circ$) and bond lengths ($<1.42 \text{ \AA}$) in pure-DLC and Ti-DLC films with Ti concentrations of 1.56 and 7.81 at.%, respectively.

many distorted C–Ti structures caused by the doping of higher Ti concentrations, the combination of these two factors can account for the increase of compressive stress shown in Fig. 3a.

4. Conclusions

In this study, AIMD simulation based on DFT was employed to study the effects of Ti impurities (1.56–7.81 at.% Ti concentrations) on the structure and properties of Ti-DLC films. When the Ti concentration increased from 0 to 1.56 at.%, the residual compressive stress in Ti-DLC film at 2.87 g/cm^3 was reduced from 17.7 to 9.4 GPa; at the density of 2.03 g/cm^3 the similar behavior of stress with the Ti concentration was also observed. By the analysis of atomic bond structure, it revealed that the stress reduction caused by Ti was attributed to both the simultaneous relaxation of distorted bond angles and bond lengths, while at higher Ti concentration the increase of distorted C–C bond lengths and the existence of distorted C–Ti structures were the key factors to result in the increased residual compressive stress.

Acknowledgments

This research was supported by the National Natural Science Foundation of China (No. 51402319, 51371187), China Postdoctoral Science Foundation (No. 2014 M551780) and Ningbo Municipal Natural Science Foundation (No. 2014A610001).

References

[1] J. Robertson, Diamond-like amorphous carbon, *Mater. Sci. Eng.* 37 (2002) 129.
 [2] N. Dwivedi, S. Kumar, J.D. Carey, R.K. Tripathi, H.K. Malik, M.K. Dalai, Influence of silver incorporation on the structural and electrical properties of diamond-like carbon thin films, *ACS Appl. Mater. Interfaces* 5 (2013) 2725.

[3] J. Wang, J. Pu, G. Zhang, L. Wang, Interface architecture for superthick carbon-based films toward low internal stress and ultrahigh load-bearing capacity, *ACS Appl. Mater. Interfaces* 5 (2013) 5015.
 [4] Z.D. Sha, V. Sorkin, P.S. Branicio, Q.X. Pei, Y.W. Zhang, D.J. Srolovitz, Large-scale molecular dynamics simulations of wear in diamond-like carbon at the nanoscale, *Appl. Phys. Lett.* 103 (2013) 073118-1.
 [5] A.H. Lettington, Applications of diamond-like carbon thin films, *Carbon* 36 (1998) 555.
 [6] C. Casiraghi, J. Robertson, A.C. Ferrari, Diamond-like carbon for data and beer storage, *Mater. Today* 10 (2007) 44.
 [7] N. Konofaos, C.B. Thomas, Characterization of heterojunction devices constructed by amorphous diamondlike films on silicon, *J. Appl. Phys.* 81 (1997) 6238.
 [8] W. Dai, P. Ke, M.W. Moon, K.R. Lee, A. Wang, Investigation of the microstructure, mechanical properties and tribological behaviors of Ti-containing diamond-like carbon films fabricated by a hybrid ion beam method, *Thin Solid Films* 520 (2012) 6057.
 [9] A.Y. Wang, K.R. Lee, J.P. Ahn, J.H. Han, Structure and mechanical properties of W-incorporated diamond-like carbon films prepared by a hybrid ion beam deposition technique, *Carbon* 44 (2006) 1826.
 [10] W. Dai, G. Wu, A. Wang, Preparation, characterization and properties of Cr-incorporated DLC films on magnesium alloy, *Diamond Relat. Mater.* 19 (2010) 1307.
 [11] K. Ma, G. Yang, L. Yu, P. Zhang, Synthesis and characterization of nickel-doped diamond-like carbon film electrodeposited at a low voltage, *Surf. Coat. Technol.* 204 (2010) 2546.
 [12] N. Dwivedi, S. Kumar, H.K. Malik, C. Sreekumar, S. Dayal, C.M.S. Rauthan, O.S. Panwar, Investigation of properties of Cu containing DLC films produced by PECVD process, *J. Phys. Chem. Solids* 73 (2012) 308.
 [13] H.W. Choi, J.H. Choi, K.R. Lee, J.P. Ahn, K.H. Oh, Structure and mechanical properties of Ag-incorporated DLC films prepared by a hybrid ion beam deposition system, *Thin Solid Films* 516 (2007) 248.
 [14] M.M.M. Bilek, D.R. McKenzie, D.G. McCulloch, C.M. Goringe, Ab initio simulation of structure in amorphous hydrogenated carbon, *Phys. Rev. B* 62 (2000) 3071.
 [15] D.G. McCulloch, D.R. McKenzie, C.M. Goringe, Ab initio simulations of the structure of amorphous carbon, *Phys. Rev. B* 61 (2000) 2349.
 [16] B. Zheng, W.T. Zheng, K. Zhang, Q.B. Wen, J.Q. Zhu, S.H. Meng, X.D. He, J.C. Han, First-principle study of nitrogen incorporation in amorphous carbon, *Carbon* 44 (2006) 962.
 [17] N.A. Marks, D.R. McKenzie, M. Bernasconi, M. Parrinello, Microscopic structure of tetrahedral amorphous carbon, *Phys. Rev. Lett.* 76 (1996) 768.
 [18] G. Kresse, J. Furthmüller, Efficiency of ab initio total energy calculations for metals and semiconductors using plane-wave basis set, *Comput. Mater. Sci.* 6 (1996) 15.
 [19] G. Kresse, J. Furthmüller, Efficient iterative schemes for ab initio total-energy calculations using a plane-wave basis set, *Phys. Rev. B* 54 (1996) 11169.
 [20] J.P. Perdew, K. Burke, M. Ernzerhof, Generalized gradient approximation made simple, *Phys. Rev. Lett.* 77 (1996) 3865.
 [21] M.J. Gillan, Calculation of the vacancy formation energy in aluminum, *J. Phys. Condens. Matter* 1 (1989) 689.
 [22] F.H. Jornada, V. Gava, A.L. Martinotto, L.A. Cassol, C.A. Perottoni, Modeling of amorphous carbon structures with arbitrary structural constraints, *J. Phys. Condens. Matter* 22 (2010) 395402-1.
 [23] R. Haerle, G. Galli, A. Baldereschi, Structural models of amorphous carbon surfaces, *Appl. Phys. Lett.* 75 (1999) 1718.
 [24] F. Li, J.S. Lannin, Radial distribution function of amorphous carbon, *Phys. Rev. Lett.* 65 (1990) 1905.
 [25] K.W.R. Gilkes, P.H. Gaskell, J. Robertson, Comparison of neutron scattering data for tetrahedral amorphous carbon with structural models, *Phys. Rev. B* 51 (1995) 12303.
 [26] X. Li, P. Ke, H. Zheng, A. Wang, Structural properties and growth evolution of diamond-like carbon films with different incident energies: a molecular dynamics study, *Appl. Surf. Sci.* 273 (2013) 670.